

Production of N₂O₅ and ClNO₂ in summer in urban Beijing, China

Wei Zhou^{1,2#}, Jian Zhao^{1,2#}, Bin Ouyang³, Archit Mehra⁴, Weiqi Xu^{1,2}, Yuying Wang⁵, Thomas J. Bannan⁴, Stephen D. Worrall^{4,a}, Michael Priestley⁴, Asan Bacak⁴, Qi Chen⁶, Conghui Xie^{1,2}, Qingqing Wang¹, Junfeng Wang⁷, Wei Du^{1,2}, Yingjie Zhang¹, Xinlei Ge⁷, Penglin Ye^{8,11}, James D. Lee⁹, Pingqing Fu^{1,2}, Zifa Wang^{1,2}, Douglas Worsnop⁸, Roderic Jones³, Carl J. Percival^{4,b}, Hugh Coe⁴, Yele Sun^{1,2,10}

¹State Key Laboratory of Atmospheric Boundary Layer Physics and Atmospheric Chemistry, Institute of Atmospheric Physics, Chinese Academy of Sciences, Beijing 100029, China

²University of Chinese Academy of Sciences, Beijing 100049, China

10 ³Department of Chemistry, University of Cambridge, Cambridge CB2 1EW, UK

⁴Centre for Atmospheric Science, School of Earth, Atmospheric and Environmental Science, University of Manchester, Manchester M13 9PL, UK

⁵College of Global Change and Earth System Science, Beijing Normal University, Beijing 100875, China

⁶College of Environmental Sciences and Engineering, Peking University, Beijing 100871, China

15 ⁷School of Environmental Science and Engineering, Nanjing University of Information Science and Technology, Nanjing 210044, China

⁸Aerodyne Research, Inc., Billerica, Massachusetts 01821, USA

⁹National Centre for Atmospheric Science, University of York, Heslington, York YO10 5DD, UK

20 ¹⁰Center for Excellence in Regional Atmospheric Environment, Institute of Urban Environment, Chinese Academy of Sciences, Xiamen 361021, China

¹¹Nanjing DiLu Scientific Instrument Inc, Nanjing, 210036, China.

^aNow at School of Materials University of Manchester, M13 9PL, UK

^bNow at Jet Propulsion Laboratory, 4800 Oak Grove Drive, Pasadena, CA 91109

[#]These authors contributed equally to this work

25 **Correspondence:** Yele Sun (sunyele@mail.iap.ac.cn) and Hugh Coe (hugh.coe@manchester.ac.uk)

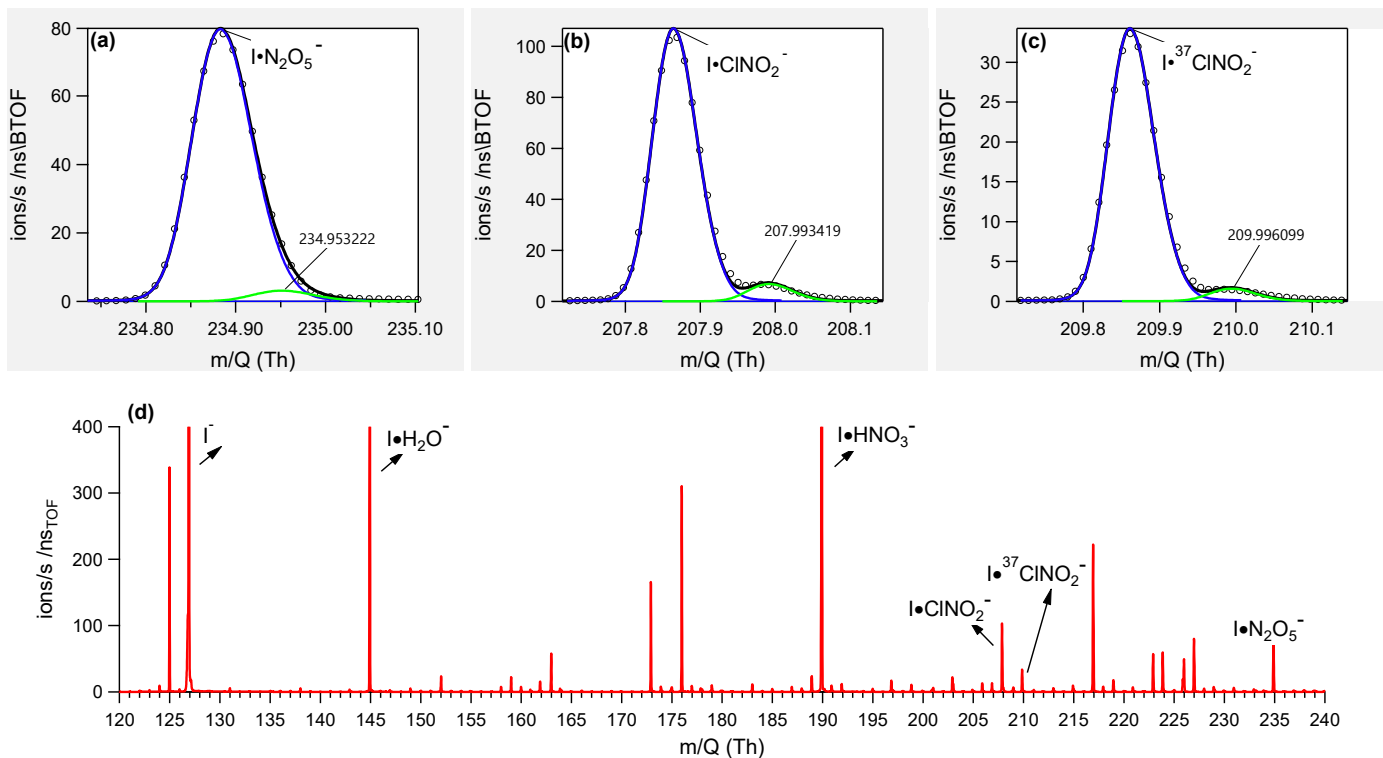


Figure S1. High resolution peak fitting for (a) m/z 235 as $I \cdot N_2O_5^-$, (b) m/z 208 as $I \cdot ClNO_2^-$, (c) m/z 210 as $I \cdot {}^{37}ClNO_2^-$, and (d) average high-resolution mass spectrum for one night from the IAP-CIMS measurement.

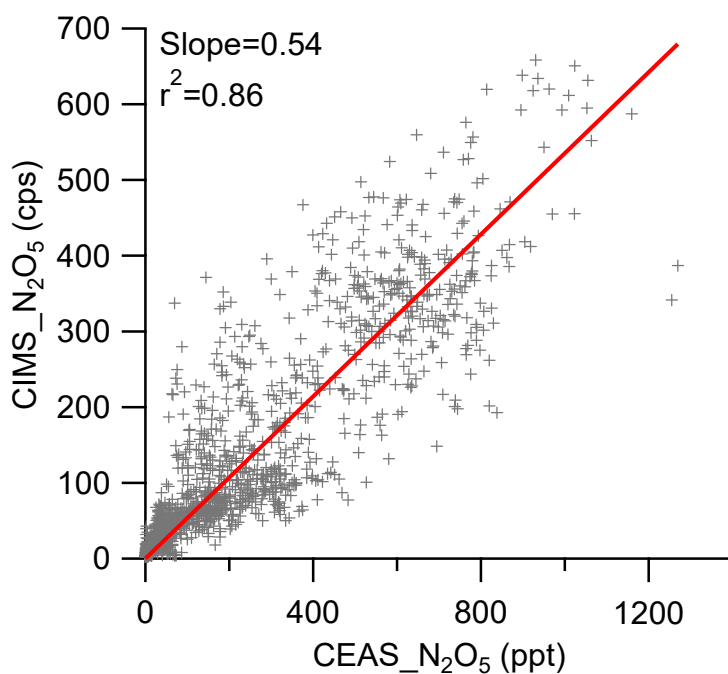


Figure S2. Comparison of IAP-CIMS raw signals of N_2O_5 with those measured by the Cambridge Broadband Cavity Enhanced Absorption Spectrometer (BBCEAS). The derived sensitivity of IAP-CIMS N_2O_5 is $0.54 \text{ cps ppt}^{-1}$.

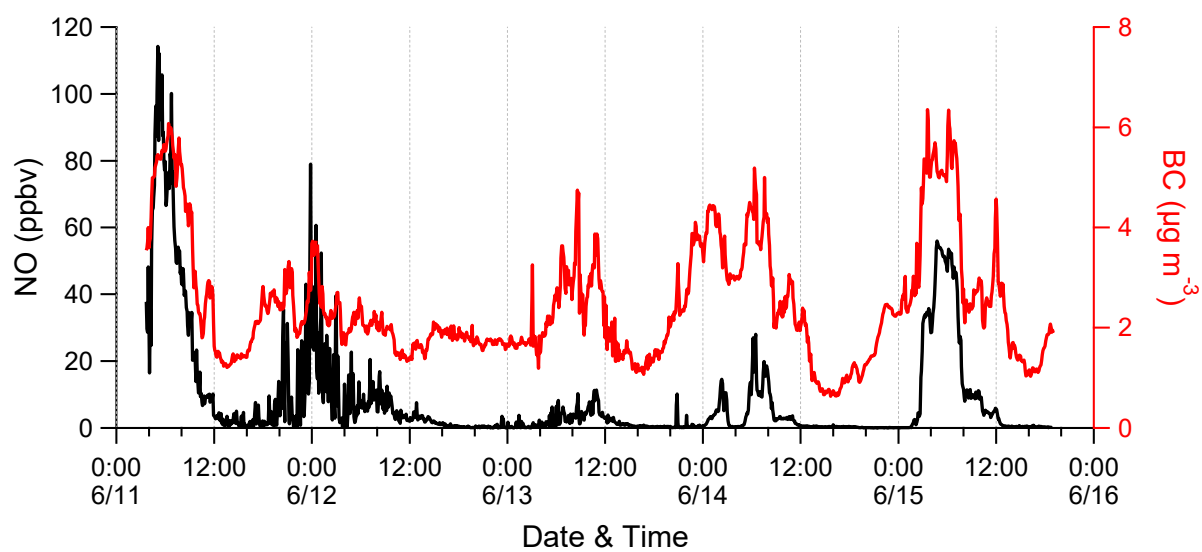


Figure S3. Time series of NO and BC during the campaign.

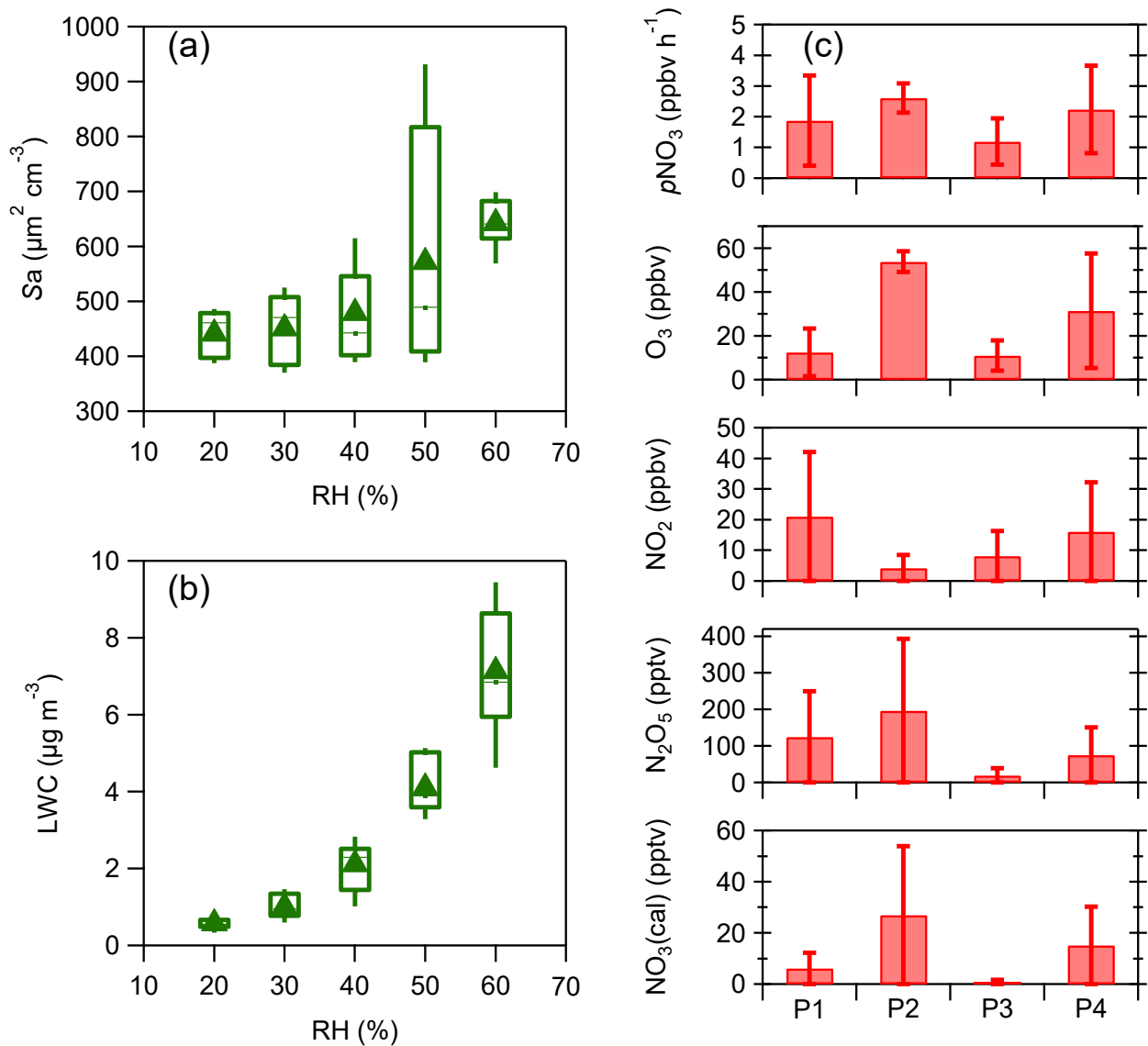


Figure S4. Variations of (a) aerosol surface area (S_a), and (b) aerosol liquid water content (LWC) as a function of RH. (c) The average mixing ratios of and NO_3 , N_2O_5 , NO_2 , O_3 and the nitrate radical production rate $p(\text{NO}_3)$ for four different nights (i.e., P1, P2, P3 and P4).

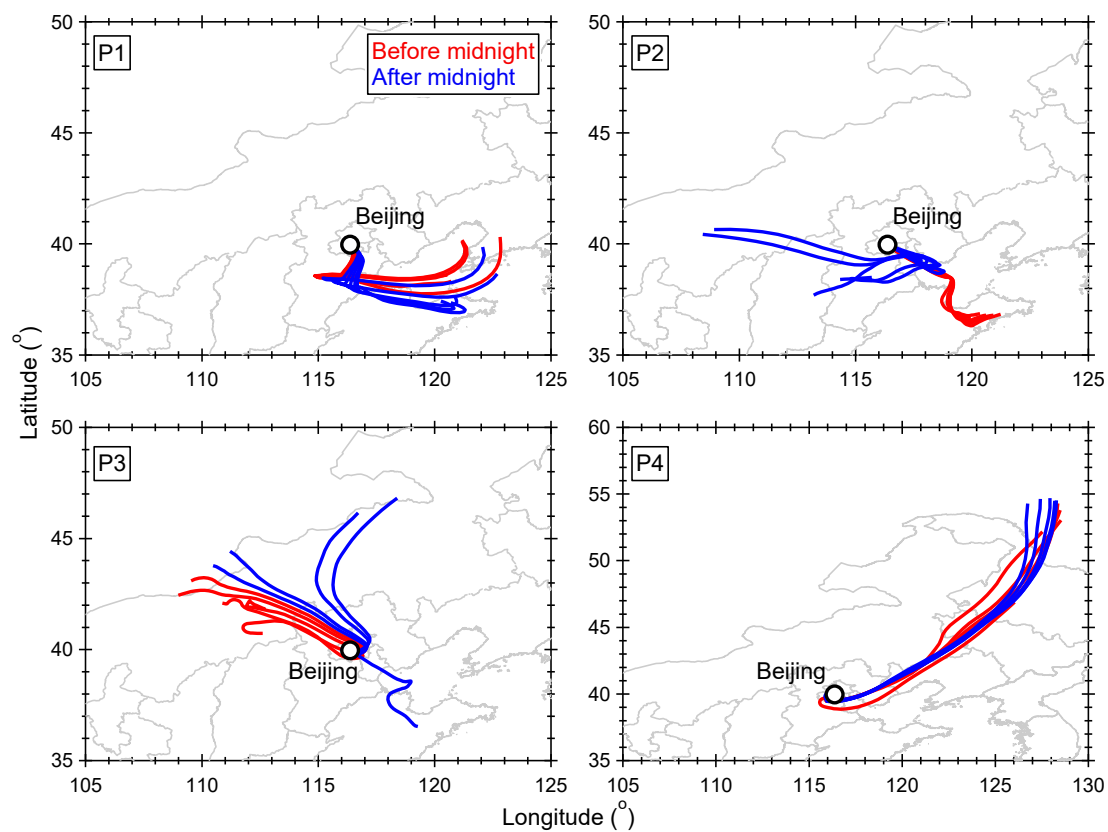


Figure S5. The 48-h back trajectories arrived at the sampling site during four different nights (i.e., P1, P2, P3 and P4). Note that the trajectories at each night are divided into two periods, i.e., before and after midnight.

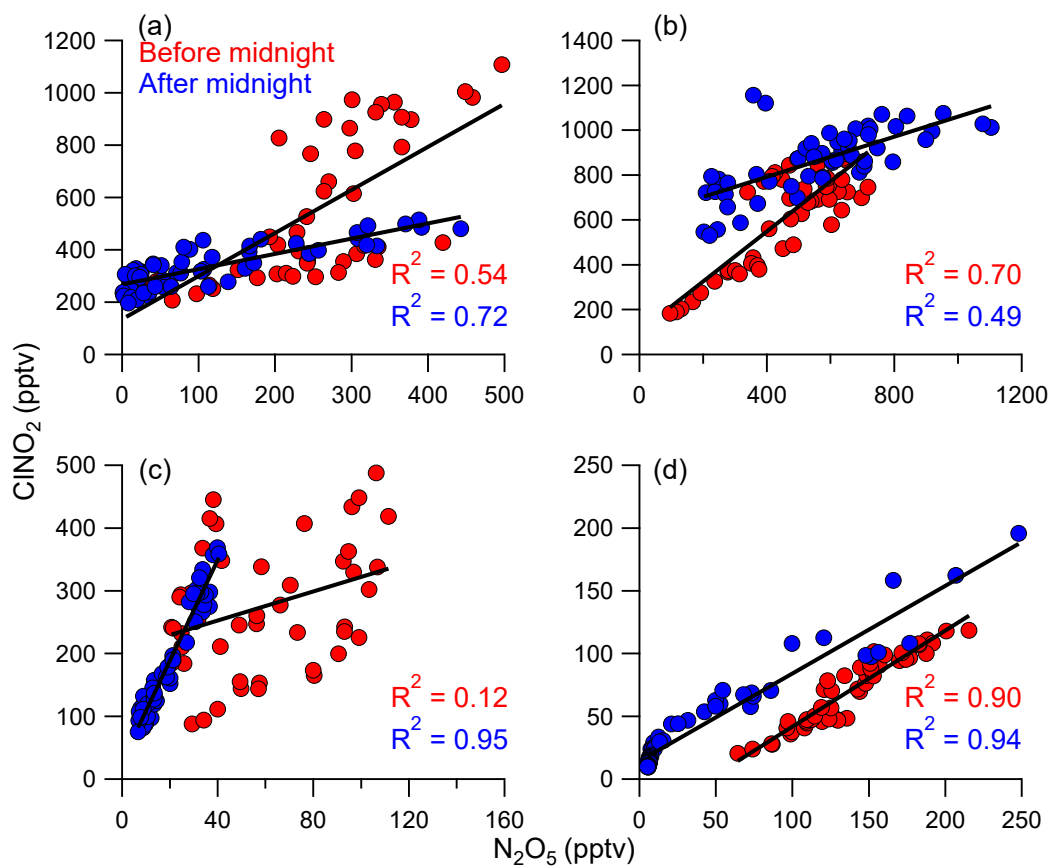


Figure S6. The correlations between ClNO_2 and N_2O_5 for four different nights (i.e., P1, P2, P3 and P4). All the correlations are divided into two periods, i.e., before midnight and after midnight.